On the Use of NCEP–NCAR Reanalysis Surface Marine Wind Fields for a Long-Term North Atlantic Wave Hindcast

VAL R. SWAIL

Environment Canada, Toronto, Ontario, Canada

ANDREW T. COX

Oceanweather, Inc., Cos Cob, Connecticut

(Manuscript received 24 August 1998, in final form 6 July 1999)

ABSTRACT

This paper uses a state-of-the-art, third-generation wave model to evaluate the marine surface wind fields produced in the National Centers for Environmental Protection–National Center for Atmospheric Research (NCEP–NCAR) Reanalysis (NRA) project. Three alternative NRA wind fields were initially considered by assessing the resulting wave hindcasts against wave measurements in the North Atlantic Ocean. The surface 10-m wind field was found to be the most skillful and was selected for further analysis.

While the wind fields from the NRA were found to be at least as skillful as the best of the analyses produced by operational Numerical Weather Prediction centers, they had significant deficiencies when compared to kinematically analyzed wind fields carried out in detailed hindcast studies. Storm peak wave heights in extratropical storms were systematically underestimated at higher sea states due to underestimation of peak wind speeds in major jet streak features propagating about intense extratropical cyclones. In addition, in situ data were incorrectly assimilated and tropical cyclones were poorly resolved.

In this study an intensive kinematic reanalysis was carried out in which wind fields in extratropical storms were intensified as necessary, in situ surface wind data were correctly reassimilated, and tropical cyclone boundary layer winds were included.

Comparisons with in situ buoy measurements and satellite altimeter data show clear improvements in both bias and scatter in the wave hindcasts using the kinematically reanalyzed wind fields, particularly in the higher sea states. Furthermore, the hindcast wind and wave climatologies closely resemble those obtained from measured wind and wave data from buoys and offshore platforms.

1. Introduction

The objective of this paper is to present an evaluation of the National Centers for Environmental Prediction–National Center for Atmospheric Research (NCEP–NCAR) global reanalysis (NRA) surface marine wind fields (Kalnay et al. 1996), in particular as the forcing of a third-generation ocean wave model adapted to the North Atlantic Ocean (NA) on a high-resolution grid. This evaluation is a part of a larger study to produce a high quality, homogeneous, long-term wind and wave database for assessment of trend and variability in the wave climate of the NA.

Since the reanalysis process itself involved, at least to some extent, the assimilation of measured surface marine data into the surface wind field products, it is not possible to derive an independent assessment of the accuracy of the NRA wind fields only from comparisons with in situ wind measurements. An alternative evaluation approach is suggested by recent studies with advanced third-generation (3-G) ocean wave prediction models (Cardone et al. 1995). Those studies show that, when such models are driven by accurate surface wind fields, nearly perfect simulations of the principal scale and shape (significant wave height and spectral peak period) properties of the surface gravity wave field result. On the other hand, if erroneous winds are used, the ocean response is modeled with obvious bias and/or scatter when compared to wave measurements. Copious high quality wave measurements have been provided within the past two decades from buoys moored near the continental margins and satellite altimeters that provide full-basin coverage. Our approach, therefore, is to hindcast the surface wave field in the North Atlantic Ocean from NRA surface marine wind fields for selected months using a proven 3-G wave model, and then to assess the quality of the wind fields through a comprehensive evaluation of the resulting wave hindcasts against all available wave measurements.

Corresponding author address: V. R. Swail, Environment Canada, 4905 Dufferin Street, Downsview, ON M3H 5T4, Canada.
E-mail: val.swail@ec.gc.ca

TABLE 1. Comparison of SWADE IOP-1 (22–31 Oct 1990) WAM-4 hindcast driven by kinematically reanalyzed wind fields against deep-water buoys in inner SWADE array.

	WS (m s^{-1})	θ (°)	SWH (m)	TP (s)
Bias	−0.05	0.6	−0.13	−0.39
rms	0.97	22	0.37	0.82
SI (%)	10	6	14	13
CC	0.99	—	0.98	0.89

Section 2 describes the basic study methodology including a description of the alternative NRA wind field products evaluated, the wave model, and the validation data. Section 3 describes the deficiencies of the NRA surface wind fields. While it was found that the NRA surface wind fields provide an unbiased background wind field for use in the production phase of the hindcast, it was found that NRA wind fields could be improved significantly by adding details of the evolution of tropical and extratropical cyclone wind field features missed in the NRA objective analyses. The enhancement process based on a comparison of eight selected months is described in section 4. This section also provides a comparative analysis of wave hindcasts from unenhanced and enhanced wind fields against high quality in situ wave measurements on both sides of the North Atlantic and basinwide altimeter measurements. Section 5 provides an evaluation of the wave height climatology derived from the enhanced wind fields at the in situ measurement sites for the first six years of production completed to date (1990–95). Section 6 gives our conclusions.

2. Evaluation methodology

a. Rationale

The recent Surface Wave Dynamics Experiment (SWADE) hindcast study (Cardone et al. 1995) suggests that when wind fields are specified accurately in a hindcast mode using intensive kinematic analysis techniques, which take advantage of the enhanced data coverage in areas of dense buoy and/or offshore platform measurement arrays (e.g., off the east and west coasts of North America and in and around the North Sea), well-calibrated wave models specify the evolution of significant wave height (SWH) with negligible bias and scatter, near the lower limit set by accuracy and sampling variability in the wave measurements. This SWADE IOP-1 11-day continuous hindcast with the WAM-4 wave model (WAMDI 1988) using kinematically reanalyzed wind fields probably best exemplifies the potential very high level of skill in contemporary wave height predictions. Table 1 gives the hindcast errors averaged over the deep-water buoys in the area of maximum SWADE data density and hence the area with the most accurate wind fields. The SWH scatter index (SI) of 14% is unprecedented for continuous hindcasts.

Errors in hindcasts validated against wave measurements on the periphery of the SWADE array increased to levels probably more typical of continuous hindcasts of midlatitude extratropical weather regimes with kinematically reanalyzed winds with an SWH SI of 18%–20%. The SWH SI was found to increase to 25%–41% in the general SWADE area when WAM-4 was driven, alternatively, by wind fields produced by operational centers. The increase in SWH SI was highly correlated with increases in wind speed (WS) SI. The lower resolution of operational wind fields is often indicted as a source of error in wave hindcasts. Graber et al. (1995) explored the effect of wind field resolution in the U.S. East Coast extratropical cyclogenetical setting of SWADE IOP-1 by making a series of sensitivity hindcasts with WAM-4, systematically degrading the spatial and temporal resolution of the reference wind fields to match approximately those of the alternative wind fields produced by the operational centers. At most buoy sites, there was little error growth between spatial resolutions of 0.5° and 1° in general and about a 25% degradation in skill at spatial resolution of 1.5°. The exception to these general conclusions was found to be at sites in the path of the main surface wind jet streak propagating about the developing cyclone, where resolutions of 0.5° and 3 h were necessary to correctly specify the storm peak sea states. Another interesting finding of this study was that wind field resolution effects alone could explain only about 20%–40% of the error observed in the alternative WAM-4 wave hindcasts made with various operational center wind fields reported by Cardone et al. (1995), leaving much of the remaining 60%–80% of the error arising caused by deficiencies in the operational center wind fields produced in October 1990 for this period.

Sterl et al. (1998) also explored the effect of model resolution in global WAM-4 hindcasts driven by winds produced by the European Centre for Medium-Range Weather Forecasts' (ECMWF's) atmospheric reanalysis of the 15-yr period 1979–93. When that hindcast was evaluated at the same National Oceanic and Atmospheric Administration (NOAA) East Coast buoys used to evaluate the deep-water SWADE hindcasts above, Sterl et al. found SWH SI in winter months of 27% when a 3° wave model grid was used and 22% when a 1.5° grid was used. They also reported a hindcast bias in SWH of −0.7 m in this area for the 3° grid and −0.5 m for the 1.5° grid. This bias was attributed mainly to underprediction of higher waves in storms.

All of the above studies highlight the close correlation between wind field errors and wave hindcast errors. Therefore, evaluation of wave hindcasts using high quality wave measurements provides a powerful way to evaluate marine wind fields.

b. Evaluation of NRA wind fields

Three alternative near-surface wind field products are available in the NRA: 1) 1000-mb wind fields available
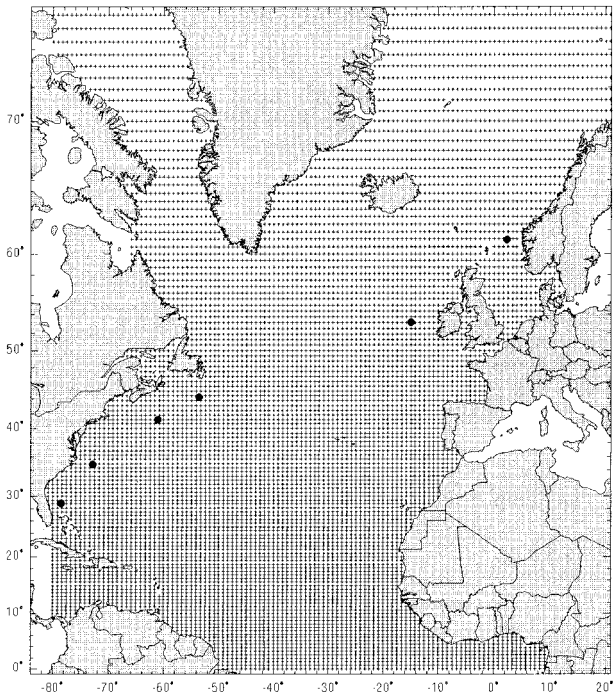
Fig. 1. OWI 3-G wave model grid for the North Atlantic Ocean and validation locations.

on the 2.5° latitude–longitude grid, 2) the lowest sigma level (0.995) wind fields on the 2.5° latitude–longitude grid, and 3) the 10-m surface wind fields on the Gaussian grid. Cox et al. (1997, 1998) showed the NRA surface 10-m wind fields produced the least biased and most skillful wave hindcasts overall, and also produced the best wind field comparisons when compared to independent wind data from *ERS-1, -2*. Further evaluation of NRA winds in this paper is restricted to this dataset.

In order to identify the deficiencies in the NRA surface 10-m wind fields eight months were chosen from the initially available period, 1979–95, for the evaluation. Months 8103 and 8301 were chosen for having the highest and lowest values, respectively, of the mean North Atlantic atmospheric zonal circulation index described by Kushnir (1994). The months 9110, 9303, and 9504 each contained extreme western North Atlantic storms hindcast in recent studies (Cardone et al. 1996; Swail et al. 1995), while 9509 was chosen as a hurricane-dominated month. The remaining months (7906, 8808) were added to provide more even representation over time of the part of the NRA available at the time this evaluation was carried out.

All wind fields for each month were interpolated from the NRA source grids onto a 0.625° by 0.833° latitude–longitude wave model grid covering the North Atlantic Ocean (Fig. 1) using the Interactive Objective Kinematic Analysis (IOKA) algorithm (Cox et al. 1995), and then time interpolated to a 1-h time step.

c. Wave model

The wave model used for this hindcast is a discrete spectral type called OWI 3-G. The spectrum is resolved at each grid point in 24 directional bins and 23 frequency bins. The bin center frequencies range from 0.039 to 0.32 Hz, increasing in geometric progression with a constant ratio 1.100 64. Deep-water physics is assumed in both the propagation algorithm and the source terms. The propagation scheme (Greenwood et al. 1985) is a downstream interpolatory scheme that is rigorously energy conserving with great circle propagation effects included. The source term formulation and integration is a third-generation type (WAMDI 1988) but with different numerics and with the following modifications of the source terms in official WAMDI. First, a linear excitation source term is added to the input source term to allow the sea to grow from a flat calm condition without an artificial warm start sea state. The exponential wind input source is taken as the Snyder et al. (1981) linear function of friction velocity, as in WAMDI. However, unlike WAM, in which friction velocity is computed from the input 10-m wind speed following the drag law of Wu (1982), a different drag law is used in OWI 3-G. That law follows Wu closely up to wind speed of 20 m s^{-1} and then becomes asymptotic to a constant at hurricane wind speeds. The dissipation source term is taken from WAMDI except that the frequency dependence is cubic rather than quadratic. Finally, the discrete interaction approximation to the nonlinear source term is used as in WAMDI except that two modes of interaction are included (in WAMDI the second mode is ignored). Further details on this model and its validation may be found in Khandekar et al. (1994), Cardone et al. (1996), and Forristall and Greenwood (1998).

OWI 3-G is adapted to the North Atlantic (NA) on a latitude–longitude grid consisting of a 122 (in lat) by 126 (in long) array of points. The grid spacing is 0.625° in latitude by 0.833° in longitude, which is within 10% of square (i.e., $\Delta x = \Delta y$) between 38° and 45°N. After deductions for land there are 9023 grid points, as shown in Fig. 1. The southern edge of the grid is at the equator, which is treated as open. Time histories of two-dimensional spectra are prescribed at all grid points along the equator as interpolated from the output of a lower-resolution global first-generation model driven by NRA 10-m wind fields. The eastern boundary is at 20°E longitude and the northern boundary is at 75.625°N latitude. The basic model integration time step is 0.5 h and consists of one 30-min propagation time step and two 15-min growth cycles.

d. Validation data

The in situ measured wind and wave data came from a variety of sources. United States buoy and C-MAN data came from the NOAA Marine Environmental Buoy Database on CD-ROM; the Canadian buoy data came

TABLE 2. Validation of North Atlantic Ocean continuous hindcasts of indicated months with OWI-3G driven by NRA 10-m surface winds compared to buoy and *ERS-1* altimeter wave measurements.

Year/Month	Variable	All buoys				*ERS-1* altimeter			
		No.	Bias	rms	SI	No.	Bias	rms	SI
9110	WS (m s^{-1})	882	0.12	2.96	0.34	16 808	0.34	2.13	0.29
	SWH (m)	758	0.01	0.77	0.24	16 703	−0.20	0.65	0.24
9303	WS (m s^{-1})	868	−0.28	2.31	0.24	17 517	0.43	2.19	0.26
	SWH (m)	871	−0.07	0.73	0.24	16 972	−0.05	0.61	0.20
9504	WS (m s^{-1})	600	−0.15	2.30	0.33	17 693	0.37	1.97	0.27
	SWH (m)	720	0.04	0.60	0.26	15 551	−0.01	0.54	0.23
9509	WS (m s^{-1})	761	0.36	2.68	0.41	18 081	0.05	2.30	0.35
	SWH (m)	834	−0.11	0.62	0.30	18 059	−0.46	0.74	0.25
All months	WS (m s^{-1})	3111	0.01	2.59	0.33	70 099	0.30	2.15	0.29
	SWH (m)	3183	−0.03	0.68	0.26	69 285	−0.18	0.64	0.23

from the Marine Environmental Data Service marine CD-ROM; the remaining data came from the Comprehensive Ocean Atmosphere Data Set (COADS). Validation sites used in this study are shown in Figure 1. The wave measurements are comprised of 20-min samples (except for Canadian buoys, which were 40 min) once per hour. The wind measurements were taken as 10-min samples, scalar averaged, except vector averaged at the Canadian buoys, also once per hour. The wind and wave values selected for comparison with the hindcast were 3-h mean values centered on each 6-h synoptic time with equal (1, 1, 1) weighting. The wind speeds were adjusted to 10-m neutral winds following the approach described in Cardone et al. (1996).

In the comparisons described in section 5, it was found that the measured datasets contained some gaps and some erroneous data. Where a gap existed in the measured data the corresponding data from the hindcast was ignored. There were many obvious spikes (high and low) in the measured data, particularly from the eastern Atlantic datasets accessed from COADS, or otherwise bad or suspicious data. These data points were removed along with the corresponding hindcast data; the amount of data removed typically was much less than 1% at the Canadian and U.S. buoy locations, and somewhat higher for the eastern Atlantic locations received through COADS. There may still remain more subtle errors in some measurements, in spite of our best efforts to identify and remove them. Removal of the hindcast data corresponding to measurements gaps is necessary to achieve a valid intercomparison between a hindcast and measurements; as a result, however, the climatologies may not be an accurate depiction of the "true" climatic conditions of the 6-yr period 1990–95.

Remotely sensed data came from both *ERS-1, -2*, and TOPEX/Poseidon instruments. *ERS-1, -2* altimeter and scatterometer measurements were extracted from Ifremer's CD-ROM set using the recommended quality controls, and then spatially binned onto the wave model grid every 6 h using a ±3-h window. TOPEX data were treated much the same as the ERS data, and the wave measurements from both instruments were adjusted as recommended by Cotton and Carter (1994).

3. Deficiencies of NRA winds

Table 2 shows the results of hindcasts using the NRA 10-m surface wind fields for four of the eight months selected (those months for which *ERS-1, -2* altimeter data are available); results for the other four months indicated similar results (not shown). The hindcasts are compared to measurements from buoys moored in deep water offshore the U.S. and Canadian east coasts and off northwestern Europe, and to the satellite data over the whole of the model domain. With respect to the buoy comparisons overall, the SWH SI of 26% indicates less skill in these hindcasts than provided by kinematically reanalyzed wind fields (see, e.g., Table 1). On the other hand, this skill is equal to or better than the best of the SWADE hindcasts driven by the wind fields from the operational centers (Cardone et al. 1995). The SWH bias of 3 cm is satisfyingly small.

The altimeter comparisons in Table 2 provide evaluation of the hindcast over the whole of the NA. These comparisons exhibit a mean difference of 18 cm and an SWH SI of 23%. Interestingly, these comparisons suggest that the skill indicated by the buoy comparisons is indicative of skill over the whole of the model domain.

Another deficiency in the NRA reanalysis concerns the assimilation of surface wind data from COADS. The assimilation scheme treated all observations at a 10-m reference level, whereas ship and drilling platform observations may actually range from about 15 m to more than 100 m, and buoy observations are typically taken about 5 m. Over the 40-yr duration of the NCEP Reanalysis this may introduce biases similar to those found by Cardone et al. (1990) due to the increasing heights of shipboard anemometers and the higher fraction of wind measurements compared to wind estimates. To overcome any potential bias in this project, all surface wind data were reassimilated after first being adjusted to the 10-m reference level.

4. Enhancement of NRA winds

a. IOKA methodology

As we have shown, the NRA surface wind fields produce wave hindcasts of good quality, but they evidently
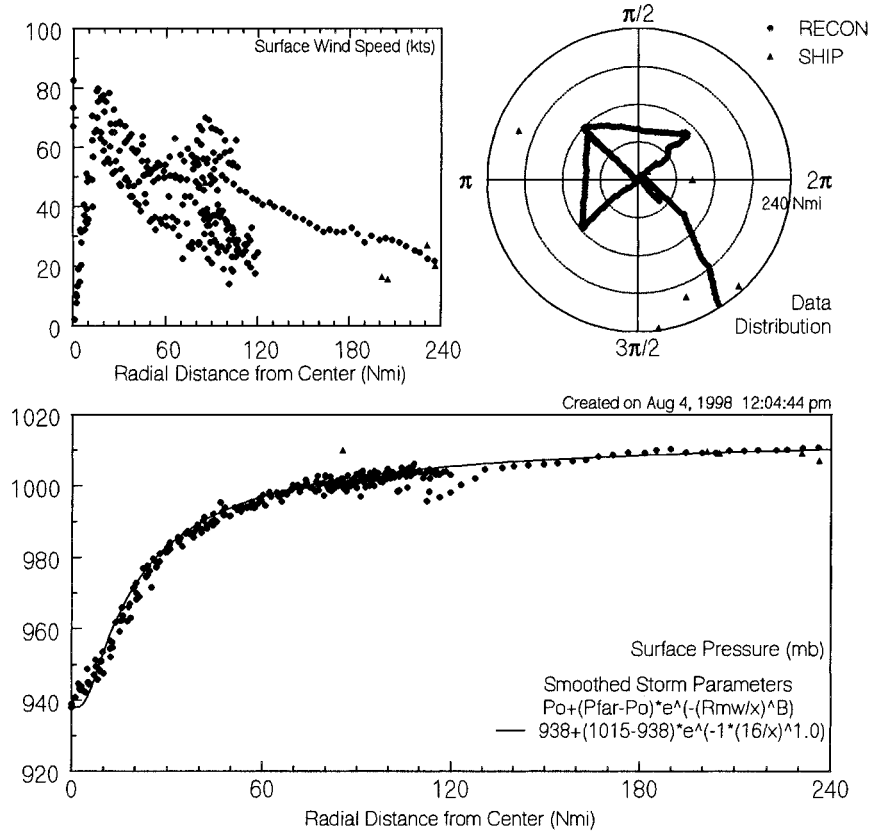
FIG. 2. Pressure model fit to aircraft reconnaissance data for Hurricane Edouard.

are susceptible of further improvement to achieve skill comparable to hindcasts driven by kinematically reanalyzed wind fields. Of particular concern was the finding that the hindcasts tended to systematically underestimate storm peaks.

Wind fields for all significant storms are kinematically reanalyzed with the aid of an interactive Wind WorkStation (Cox et al. 1995). The NRA surface wind fields are brought into the Wind WorkStation every 6 h in monthly segments for evaluation by a trained marine
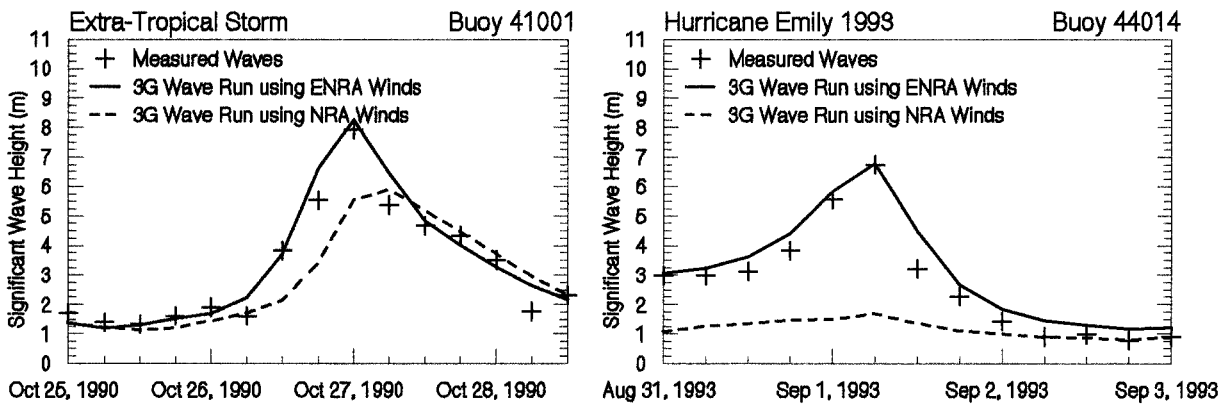

FIG. 3. Effect of kinematic analysis on the wave hindcast for an extratropical storm (left) and a tropical storm (right).
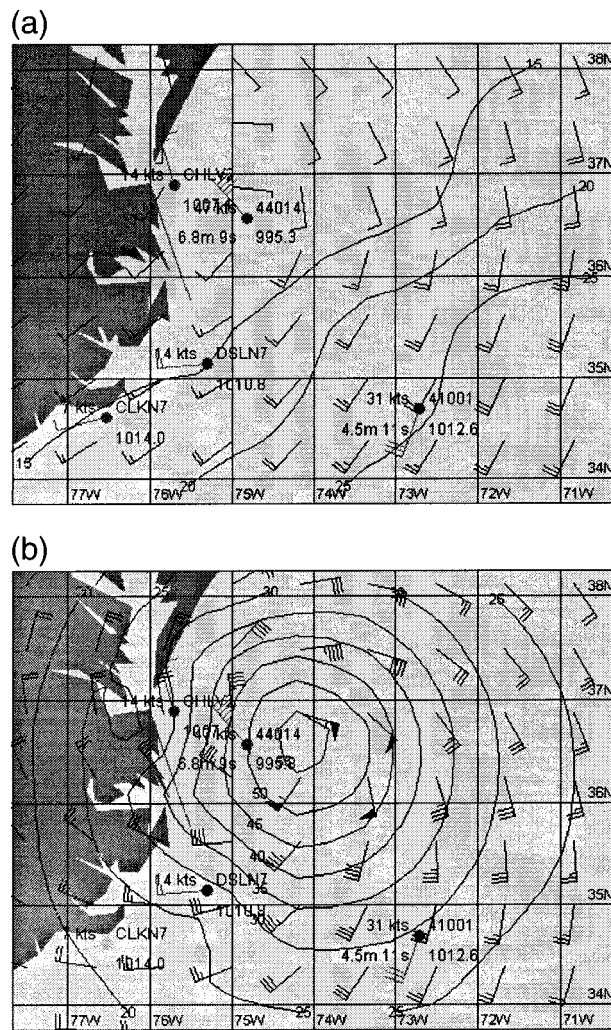
(a)

(b)

FIG. 4. Surface wind fields for Hurricane Emily for (a) NRA and (b) ENRA wind fields with tropical vortex model winds incorporated.
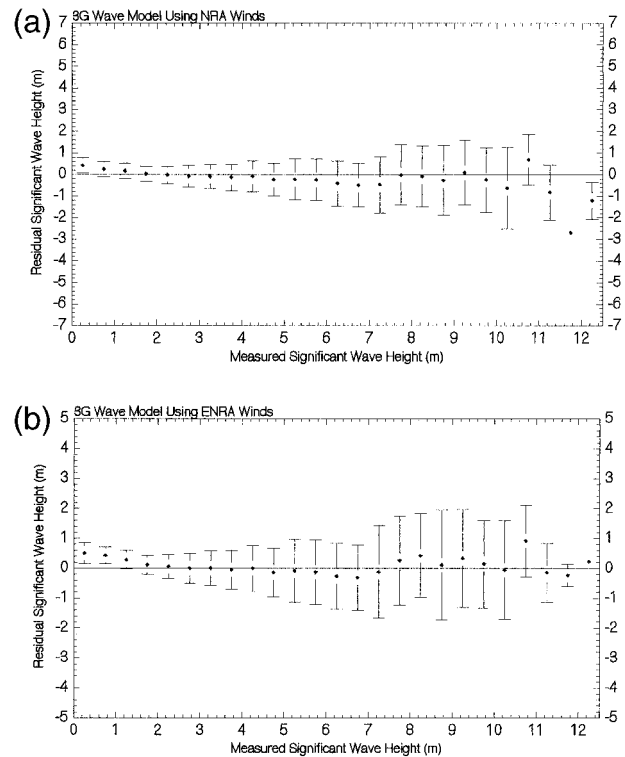
(a)

(b)

FIG. 5. (a) Comparison of the hindcast from NRA winds and *ERS-1* altimeter in 0.5-m altimeter bins of SWH (bins with fewer than five comparisons are not shown) for one of the four months evaluated, Mar 1993. In each bin we plot the mean difference and the standard deviation of the difference for all comparison pairs within the bin. (b) Same comparison as (a) except that ENRA winds were used for the hindcast.

meteorologist. The NRA surface winds are further refined by computing an equivalent neutral wind using the NRA 2-m surface temperature and sea surface temperature fields and the algorithm described by Cardone et al. (1990). To remove potential biases in the historical wind fields, all wind observations including buoy observations, ship reports (from COADS), and C-MAN stations are reassimilated into the analysis taking ac-

TABLE 3. Validation of North Atlantic Ocean continuous hindcasts with OWI-3G driven by ENRA winds compared to buoy and *ERS-1* altimeter wind speed and wave height measurements.

		All buoys				*ERS-1* altimeter			
Year/Month	Variable	No.	Bias H–M	rms	SI	No.	Bias H–M	rms	SI
9110	WS	882	0.69	2.41	0.26	16 808	0.39	2.19	0.30
	SWH	758	0.26	0.76	0.25	16 703	−0.06	0.64	0.25
9303	WS	868	0.19	1.04	0.11	17 517	0.46	2.26	0.27
	SWH	871	0.09	0.68	0.22	16 972	0.05	0.63	0.21
9504	WS	600	−0.05	1.85	0.09	17 693	0.38	1.94	0.27
	SWH	720	0.11	0.55	0.22	17 551	0.07	0.53	0.22
9509	WS	761	0.42	1.28	0.19	18 081	0.13	2.20	0.34
	SWH	834	0.09	0.53	0.26	18 059	−0.23	0.60	0.24
All months	WS	3111	0.40	1.73	0.17	70 099	0.39	2.15	0.29
	SWH	3183	0.13	0.64	0.24	69 285	−0.04	0.60	0.23

TABLE 4. Comparison of climatological statistics for the ENRA wind driven wave hindcasts at selected locations for the period 1990–95.

	HS model (m)	HS meas (m)	WS model (m s^{-1})	WS meas (m s^{-1})
62108				
Mean	3.44	3.32	9.94	9.94
Std dev	1.82	1.87	4.53	4.62
Coef_var	0.53	0.56	0.46	0.46
Skew	1.45	1.36	0.49	0.48
Max	13.55	13.50	33.78	34.45
90% ILE	5.83	6.00	15.89	15.92
95% ILE	6.86	7.00	17.77	17.84
99% ILE	9.64	9.70	22.03	22.11
LF3J				
Mean	3.19	2.87	9.71	8.96
Std dev	1.84	1.70	4.67	4.77
Coef_var	0.57	0.59	0.48	0.53
Skew	1.21	1.04	0.69	0.68
Max	11.89	12.00	32.08	30.05
90% ILE	5.70	5.00	16.16	15.52
95% ILE	6.72	6.00	18.49	17.80
99% ILE	9.11	8.00	22.23	21.80
41001				
Mean	1.96	1.96	7.69	7.55
Std dev	1.02	1.08	3.52	3.56
Coef_var	0.52	0.55	0.46	0.47
Skew	1.89	1.72	0.64	0.51
Max	9.27	10.00	23.60	23.89
90% ILE	3.28	3.47	12.51	12.39
95% ILE	3.99	4.10	14.32	14.03
99% ILE	5.45	5.63	17.12	16.92
41010				
Mean	1.66	1.56	6.48	6.51
Std dev	0.79	0.83	3.08	3.13
Coef_var	0.47	0.53	0.47	0.48
Skew	1.72	1.64	0.64	0.59
Max	8.36	7.53	23.10	23.03
90% ILE	2.72	2.67	10.66	10.75
95% ILE	3.21	3.23	12.16	12.26
99% ILE	4.36	4.43	14.80	14.84
44137				
Mean	2.65	2.58	9.11	8.99
Std dev	1.50	1.55	4.35	4.45
Coef_var	0.57	0.60	0.48	0.50
Skew	1.95	1.86	0.53	0.45
Max	15.09	15.80	28.73	28.38
90% ILE	4.51	4.57	15.08	15.09
95% ILE	5.49	5.63	16.87	16.98
99% ILE	8.12	7.90	20.38	20.27
44138				
Mean	2.69	2.67	8.67	8.57
Std dev	1.47	1.54	4.18	4.18
Coef_var	0.55	0.58	0.48	0.49
Skew	2.05	1.77	0.70	0.57
Max	13.43	13.40	29.27	26.35
90% ILE	4.52	4.65	14.40	14.21
95% ILE	5.46	5.66	16.27	16.21
99% ILE	8.36	8.00	20.16	19.84

count of the method of observation, anemometer height, and stability. *ERS-1, -2* scatterometer winds are displayed and selectively assimilated (as determined by the analyst) into the final wind field.

The interactive hindcast methodology used by the analysts follows similar previous hindcast studies (Cardone et al. 1995, 1996). Particular attention is spent on strong extratropical systems and the quality control of surface data. Kinematically analyzed winds from previous hindcasts of severe extratropical storms in the northwest Atlantic (Swail et al. 1995) are incorporated into the present analysis on the North Atlantic wave model grid.

Altimeter measurements are used in an inverse wave-modeling approach as follows. First, a global coarse wave run is made and hindcast wave heights over the North Atlantic Ocean are compared to altimeter wave measurements. The global wave fields are generated using Oceanweather's 1-G wave model (Khandekar et al. 1994) adapted to a 1.25° by 2.5° latitude–longitude grid for the entire globe. NRA surface winds (adjusted to neutral stability) are used to drive the global wave model. Areas where the resulting wave fields are deficient, as indicated by the altimeter, are brought to the analysts' attention, and the analyst subjectively rectifies the deficiencies in the backward space–time evolution of the wind field causing the discrepancy.

b. Inclusion of tropical systems

It was also found in the NRA hindcasts that tropical storms are poorly resolved in the NRA wind fields. High-resolution surface wind fields for all tropical cyclones, as specified by a proven tropical cyclone boundary layer model (Cardone et al. 1994; Thompson and Cardone 1996), are assimilated into the wind fields to provide greater skill and resolution in the resulting wave hindcasts. Track and initial estimates of intensity are taken, with some modification, from the NOAA Tropical Prediction Center's (TPC) HURDAT database. The radius of maximum wind is determined using a pressure profile fit to available surface observations and aircraft reconnaissance data. Reconnaissance data are taken from TPC's Annual Data and Verification Tabulation diskettes from 1989 to 1996, digitally scanned from manuscript records for the period 1974–88, and manually scanned from reconnaissance microfilm for periods prior to 1974. Figure 2 shows a pressure model fit to reconnaissance data adjusted to the surface via Jordan (1958). Surface winds generated from the model are then evaluated against available surface data and aircraft reconnaissance wind observations adjusted to the surface as described by Powell and Black (1990). Model winds within 240 nmi from the center are then exported on a 0.5° latitude–longitude grid for inclusion and blending using the Wind WorkStation.
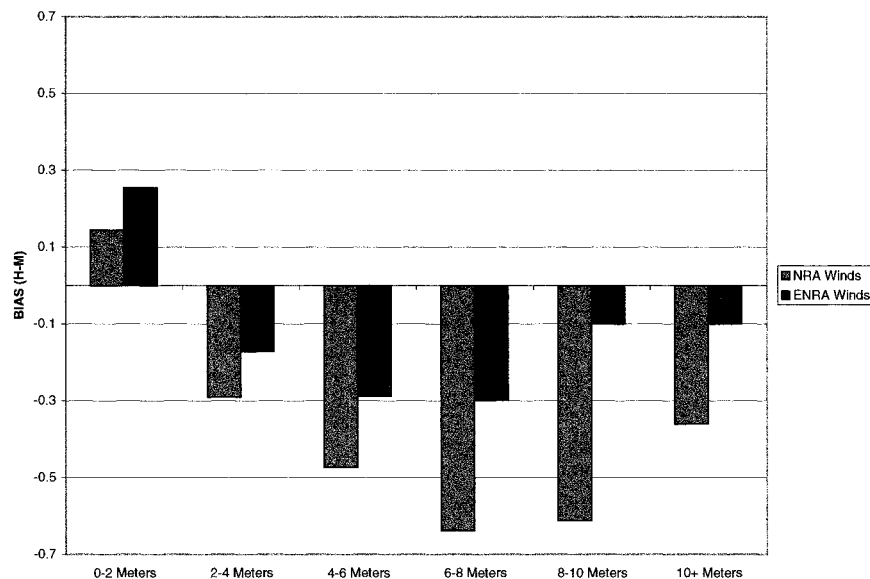
FIG. 6. Wave model grid averaged altimeter wave measurements binned every 2 m compared with the matching hindcast waves within ±3 h (H–M) showing the mean bias for each bin over all evaluation months.

c. Comparison of high-frequency wind and wave results

Figure 3 (left) shows the hindcast made with NRA surface winds at a buoy off the U.S. East Coast during SWADE IOP-1 and the hindcast made after the NRA winds are kinematically enhanced (hereafter ENRA) with the aid of an interactive Wind WorkStation. This case is typical of the improvement in skill of the hindcast overall and the reduction in the underestimation of storm peaks when the NRA surface wind fields are reanalyzed.

Figure 4 compares the NRA and ENRA winds during Hurricane Emily (September 1993). The improvement is achieved through a combination of interactive kinematic analysis of the wind fields in conjunction with winds generated by a proven tropical cyclone model. The resulting wave comparison at buoy 44014 is shown in Fig. 3 (right panel).

Table 3 shows the validation of the hindcasts against buoy and altimeter data for hindcasts made using the ENRA wind fields for the same four months shown in Table 2. At the buoys there is a significant reduction in the scatter index for wind speed, nearly a factor of 2 reduction over all buoys, which is to be expected because the buoys winds have been reassimilated at the correct height. The wave height SI is reduced as well but by only about 10% overall. Altimeter wind speeds and wave heights are not assimilated so the altimeter statistics give an independent measure of skill in the hindcasts. By comparing Tables 2 and 3 it is seen that there is no significant difference in the scatter statistics between runs made with NRA and ENRA winds. This result is not surprising since the scatter statistics are dominated by lower sea states, which would not be

changed substantially by the IOKA process. However, there is a reduction of the wave height bias overall from 18 to 4 cm. This reduction in bias is mainly contributed by increased skill in specification of a storm-generated sea state, as shown, for example, in Figs. 5a,b. Figure 5a compares the hindcast from NRA winds and *ERS-1* altimeter in 0.5-m altimeter bins of SWH (bins with fewer than five comparisons are not shown) for one of the four months evaluated. Figure 5b shows the same comparison except that ENRA winds were used for the hindcast. In each bin we plot the mean difference and the standard deviation of the difference for all comparison pairs within the bin. At lower sea states the comparisons based on the NRA and ENRA winds are nearly the same, while at higher sea states the enhanced winds provide more skillful hindcasts. Similar plots for the other comparison months and TOPEX altimeter measurements (not shown) indicate the tendency for improvement overall and significant improvement at the higher sea states.

Figure 6 shows the wave model grid-averaged altimeter wave measurements binned every 2 m compared with the matching hindcast waves (within ±3 h), showing the mean bias for each bin over the four evaluation months. While the buoy comparisons indicate the skill in the hindcasts near the continental margins, the altimeter samples the entire North Atlantic basin more or less evenly in space and time. It is encouraging, therefore, that wave hindcasts show very good agreement with the altimeter throughout the range of wave heights. The mean in bias in wave height derived from the ENRA winds over the four months is within ±30 cm, while the NRA analysis had biases nearly twice that value.
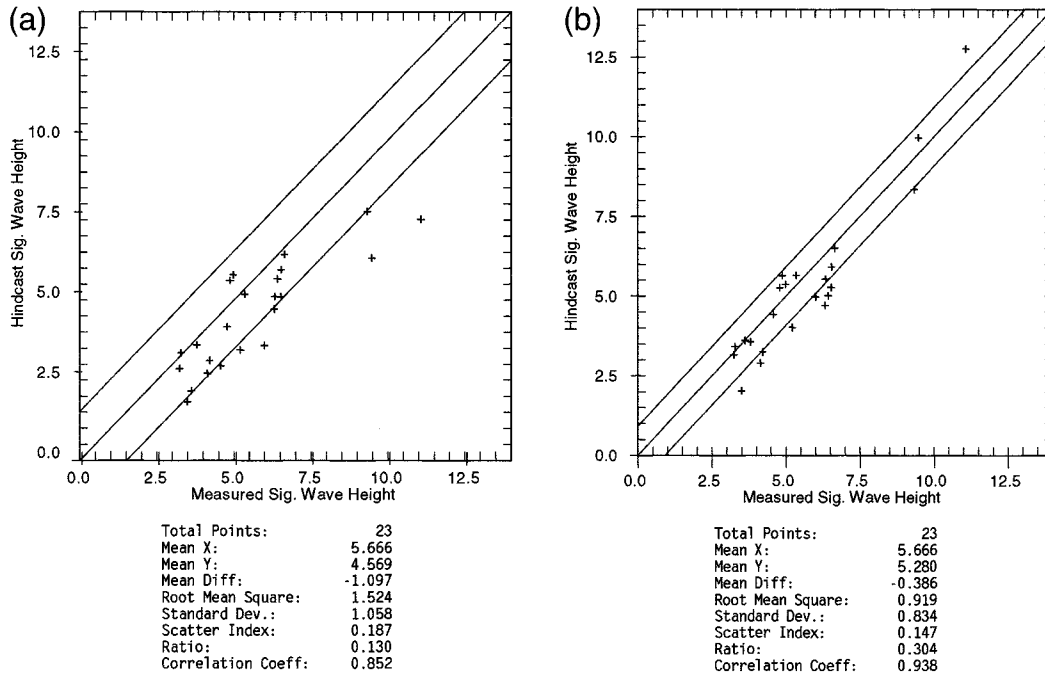
Total Points:	23
Mean X:	5.666
Mean Y:	4.569
Mean Diff:	-1.097
Root Mean Square:	1.524
Standard Dev.:	1.058
Scatter Index:	0.187
Ratio:	0.130
Correlation Coeff:	0.852

Total Points:	23
Mean X:	5.666
Mean Y:	5.280
Mean Diff:	-0.386
Root Mean Square:	0.919
Standard Dev.:	0.834
Scatter Index:	0.147
Ratio:	0.304
Correlation Coeff:	0.938

Fig. 7. Comparison of peak-to-peak wave height using (a) NRA and (b) ENRA wind fields to drive 3-G wave models for four months.
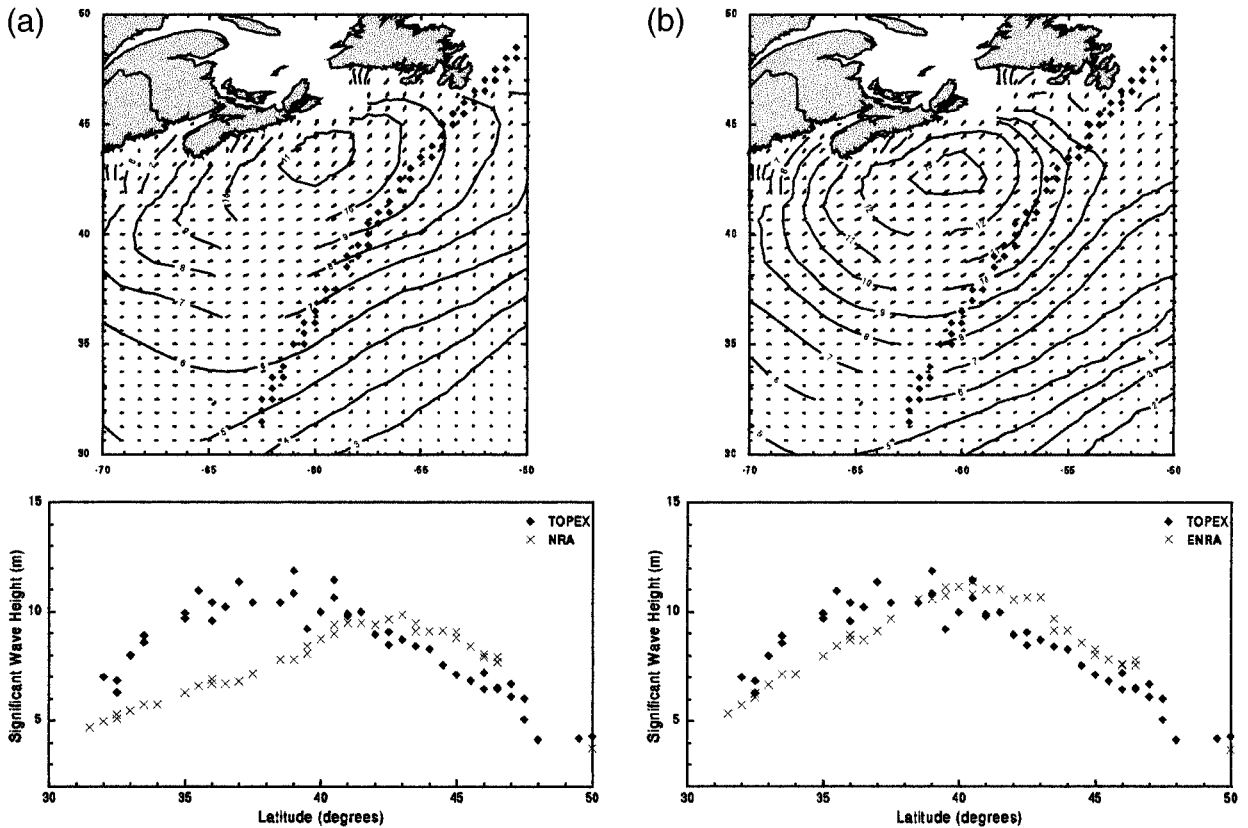
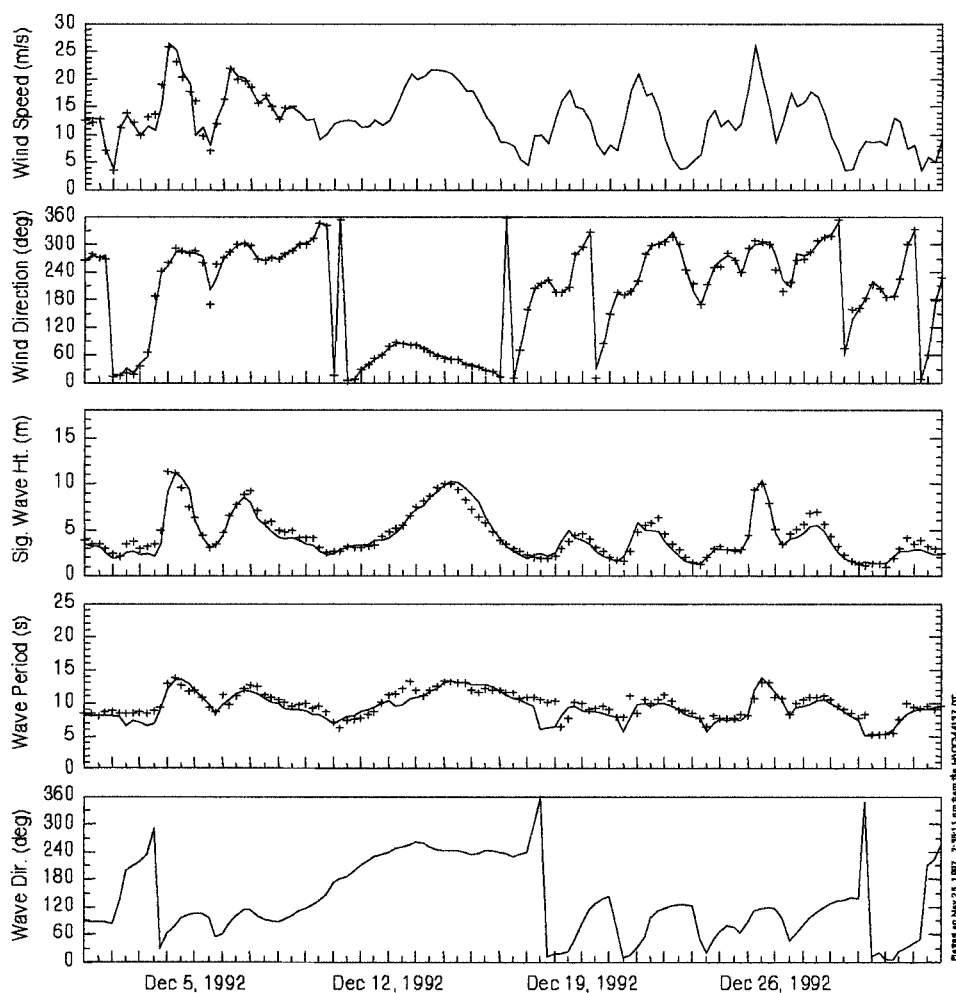Fig. 8. Comparison of TOPEX altimeter wave measurements vs (a) NRA and (b) ENRA modeled waves.

FIG. 9. Time series comparison of hindcast (solid line) and measured winds and waves at Canadian buoy 44137 during Dec 1992 using ENRA wind fields.

Hindcast wave heights less than 1.5 m show a slight systematic overestimation, which may be attributed to a natural tendency for the gridded wind and wave fields to fail to resolve small areas of calm winds and seas.

Given the emphasis in the ENRA on specification of storm wind fields, it is interesting to compare the production wave hindcasts with wave hindcasts made with the NRA surface winds during storm peaks. Figure 7 shows the comparison of storm peaks greater than 3 m (as measured by the buoy) at buoy 44138 for the four overlapping evaluation and production months. This figure shows a clear reduction in both the bias and scatter when using the ENRA wind fields.

In Figure 8 TOPEX altimeter wave measurements along a swath are compared in an extratropical storm off the east coast of Canada. The improvements resulting from the ENRA winds are clearly evident along the TOPEX track; the figure shows that not only does the ENRA capture more accurately the peak of the storm but also the spatial characteristics of the wave field.

Figure 9 shows a typical example of the time series comparison of wind speed, wind direction, wave height, wave period, and wave direction for buoy 44137 during December 1992. The excellent agreement in the winds is a consequence of the IOKA, which has naturally assimilated the buoy observation into each 6-hourly analysis. The buoy wave height and period (there is no wave direction measurement at this buoy) time series, however, provides an independent assessment of the wave hindcast.

5. Representation of wind and wave climatology

Comparisons of the ENRA wind and wave climatology at six buoys and platforms selected to give a comprehensive geographical coverage over the North Atlantic Ocean, well away from the coast, in deep water, were carried out for the period 1990–95.

The hindcast and measured wind speed climatologies are not independent since all of the wind data used contributed heavily to the data assimilation scheme in the NCEP reanalysis and again in the kinematic re-
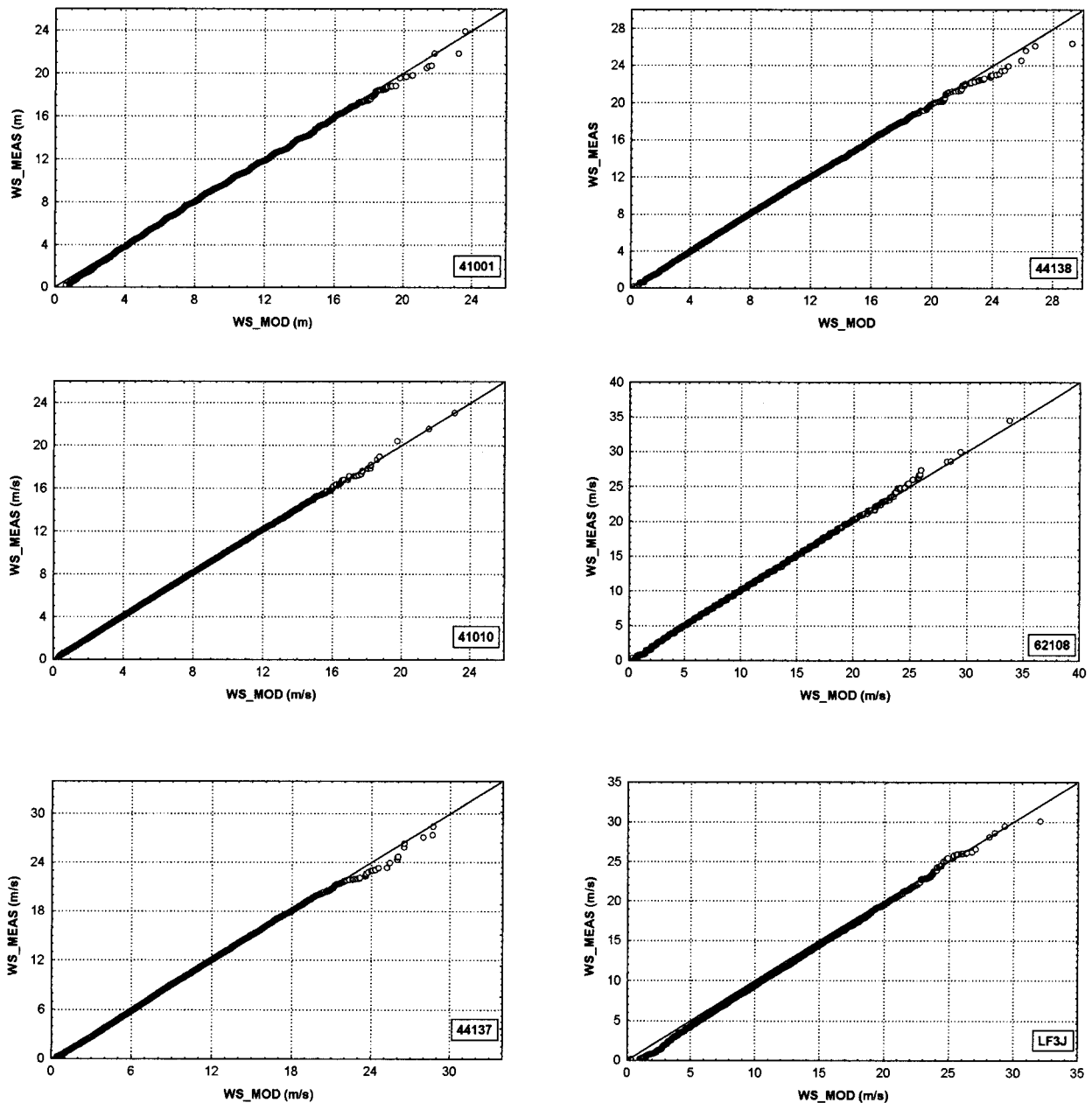
FIG. 10. Quantile–quantile plots of wind speed for selected measurement locations based on ENRA-driven hindcasts.

analysis. Nevertheless, it is useful to compare the two datasets to verify that the various adjustments for elevation and interpolation onto the wave model grid have not compromised the hindcast dataset.

Table 4 shows that the mean wind speeds are within a few centimeters per second, except at the Gullfaks platform (LF3J), where the differences are about 0.6–0.7 m s^{-1}; the model mean winds were generally equal to or slightly higher than the measurements at all locations. The wind speed standard deviations were quite similar with the measured winds being slightly more variable. The higher-order moments were also compa-

rable, with the hindcast having consistently higher values of skewness. The 90, 95, and 99 percentile wind speeds were nearly identical, although the model winds at the platform was 0.6–0.7 m s^{-1} higher than the measurements. There were some differences in the maximum wind speeds, split evenly between the two data sources as to which was higher. Differences were typically on the order of 2–3 m s^{-1}.

Figure 10 shows quantile–quantile (Q–Q) plots for model versus measured wind speed for each of the six selected sites. The Q–Q plots illustrate the comparison of the full frequency distributions, particularly in the
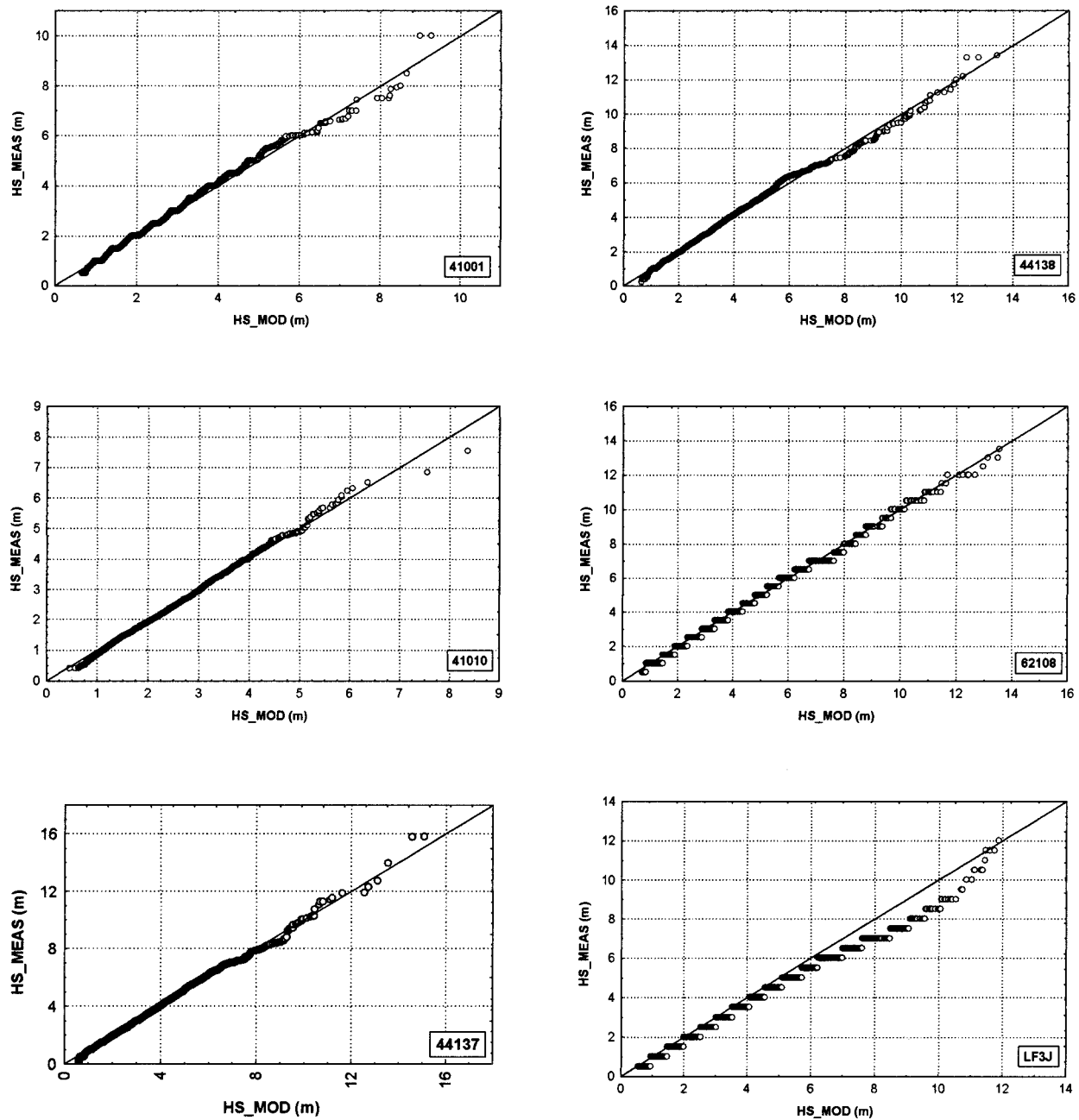
FIG. 11. Quantile–quantile plots of significant wave height for selected measurement locations based on ENRA-driven hindcasts.

right-hand (extreme) tails. These plots show very good agreement across the entire frequency distribution. There is a tendency for the ENRA winds to be slightly higher at the Canadian buoys, particularly for the highest wind speeds, which is possibly related to the vector averaging of the buoy wind samples as opposed to scalar averages elsewhere. At the platform the model is noticeably higher than the measurements for the low end of the wind speed distribution.

It is also clear from Table 4 that the hindcast represents the wave climate very well at the selected loca-

tions. The hindcast mean wave heights typically exceed the measurements by a few centimeters. The standard deviations are also very closely approximated, with the buoy measurements being slightly more variable than the hindcasts, and the platforms slightly lower. The higher-order moments of the distribution are also remarkably close. The 90, 95, and 99 percentile wave heights are typically within a few centimeters at the buoys, with the measurements tending usually to be slightly higher than the hindcasts; at the platform the model is noticeably higher than the measurements.

Comparisons of the maximum hindcast and measured waves show no clear pattern. In some cases the measurements are higher, most notably at 44137 where the 15.8 m maximum came from the Halloween storm documented by Cardone et al. (1996), which showed an inability of all the models tested to reproduce the extreme wave heights generated by the storm. Generally, the differences in the wave height maxima were less than 1 m.

Figure 11 shows Q–Q plots for model versus measured wave height for each of the six selected sites. These plots show very good agreement across the entire frequency distribution. There is a slight tendency for the model to overestimate the wave height compared to the measurements for low values of sea state. The model also is consistently higher at the platform, although the differences are negligible for the few highest observations. The effect of the Halloween storm is clearly seen at 44137 and 44138, where the peak measured waves clearly exceed the hindcast values. The Gullfaks platform does not strictly satisfy the conditions of deepwater open ocean; a model of much higher grid resolution would be required to properly describe the propagation of wave energy from the North Atlantic Ocean into the North Sea through the British Isles.

6. Conclusions

The evaluation of wave hindcasts using high quality wave measurements provides a powerful way to evaluate marine surface wind fields. In this paper, the NRA surface 10-m wind fields were used to drive a 3-G wave model and were shown to produce wave hindcasts of good quality, relatively unbiased with low scatter index compared to buoys and satellite altimeter.

However, it was also found from our evaluation of wave hindcasts driven by the surface 10-m wind fields that the winds suffered from several major deficiencies. First, storm peak wave heights in extratropical storms were systematically underestimated at higher sea states. This was result of the underestimation of peak wind speeds in major jet-streak features propagating about intense extratropical cyclones. Second, tropical cyclone wind fields were not only poorly resolved (as expected on a coarse global grid) but often did not even display sufficient energy at the grid resolution of the NRA model. Furthermore, in situ surface marine observations were assimilated into the NRA wind fields without regard to differences in averaging interval and anemometer level, a practice that may introduce a potential bias.

In this study, NRA surface winds were reanalyzed and enhanced with the aid of analyst-interactive techniques, during which in situ data were correctly reassimilated, wind fields in extratropical storms were intensified as necessary, and tropical cyclone boundary layer winds were included. Consistent with where the enhancement effort was concentrated, we found that the main difference between the NRA and ENRA hindcasts was in a more accurate specification of storm seas (SWH > 6 m). Because the proportion of sea states above this threshold was quite small, we did not see a significant reduction in the typical global measures of skill used by modelers, such as mean error and scatter index based on the whole hindcast population. Evaluation of wave hindcasts driven by the ENRA wind fields against all buoy measurements over the eight evaluation months showed a significant improvement in specification of storm peaks. Evaluation of wave hindcasts driven by the enhanced wind fields against altimeter wave height measurements over the four months evaluated showed a reduction in bias from −0.18 to −0.04 m.

The wind speed and wave height climatology produced from the hindcast using kinematically analyzed wind fields closely resembles that obtained from measured wind and wave data from buoys and offshore platforms on both sides of the Atlantic Ocean, in terms of the various statistical moments and the shape and scale of mainly the frequency distributions. This confirms that the wave hindcast results may be used as a high quality estimate of the actual wave climate.

REFERENCES

Cardone, V. J., J. G. Greenwood, and M. A. Cane, 1990: On trends in historical marine wind data. *J. Climate,* **3,** 113–127.
——, A. T. Cox, J. A. Greenwood, and E. F. Thompson, 1994: Upgrade of tropical cyclone surface wind field model. U.S. Corps of Engineers Misc. Paper CERC-94-14, 97 pp. [Available from NTIS, 5295 Port Royal Road, Springfield, VA 22161.]
——, H. C. Graber, R. E. Jensen, S. Hasselmann, and M. J. Caruso, 1995: In search of the true surface wind field in SWADE IOP-1: Ocean wave modelling perspective. *Global Ocean Atmos. Syst.,* **3,** 107–150.
——, R. E. Jensen, D. T. Resio, V. R. Swail, and A. T. Cox, 1996: Evaluation of contemporary ocean wave models in rare extreme events: ''Halloween Storm'' of October 1991 and the ''Storm of the Century'' of March 1993. *J. Atmos. Oceanic Technol.,* **13,** 198–230.
Cotton, P. D., and D. J. T. Carter, 1994: Cross calibration of TOPEX, *ERS-1,* and Geosat wave heights. *J. Geophys. Res.,* **99,** 25 025–25 033.
Cox, A. T., J. A. Greenwood, V. J. Cardone, and V. R. Swail, 1995: An interactive objective kinematic analysis system. *Proc. Fourth Int. Workshop on Wave Hindcasting and Forecasting,* Banff, AB, Canada, Atmospheric Environment Service, 109–118.
——, V. J. Cardone, and V. R. Swail, 1997: Evaluation of NCEP/NCAR reanalysis project marine surface wind products for a long term North Atlantic wave hindcast. *Proc. First WCRP Int. Conf. on Reanalyses,* Silver Spring, MD, WMO, 73–76.
——, ——, and ——, 1998. Evaluation of NCEP/NCAR reanalysis project marine surface wind products for a long term North Atlantic wave hindcast. *Proc. Fifth Int. Workshop on Wave Hindcasting and Forecasting,* Melbourne, FL, Atmospheric Environment Service, 30–40.

Forristall, G. Z., and J. A. Greenwood, 1998: Directional spreading of measured and hindcasted wave spectra. *Proc. Fifth Int. Workshop on Wave Hindcasting and Forecasting,* Melbourne, FL, Atmospheric Environment Service, P5–P15.

Graber, H. C., R. E. Jensen, and V. J. Cardone, 1995: Sensitivity of wave model predictions on spatial and temporal resolution of the wind field. *Proc. Fourth Int. Workshop on Wave Hindcasting and Forecasting,* Banff, AB, Canada, Atmospheric Environment Service, 263–278.

Greenwood, J. A., V. J. Cardone, and L. M. Lawson, 1985: Intercomparison test version of the SAIL wave model. *Ocean Wave Modelling,* Plenum Press, 221–233.

Jordan, C. L., 1958: Estimation of surface central pressures in tropical cyclones from aircraft observations. *Bull. Amer. Meteor. Soc.,* **39,** 345–352.

Kalnay, E., and Coauthors, 1996. The NCEP/NCAR 40-year reanalysis project. *Bull. Amer. Meteor. Soc.,* **77,** 437–471.

Khandekar, M. L., R. Lalbeharry, and V. J. Cardone, 1994: The performance of the Canadian Spectral Ocean Wave Model (CSOWM) during the Grand Banks *ERS-1* SAR Wave Spectra Validation Experiment. *Atmos.–Ocean,* **31,** 31–60.

Kushnir, Y., 1994: lnterdecadal variations in North Atlantic sea surface temperature and associated atmospheric conditions. *J. Climate,* **7,** 141–157.

Powell, M. D., and P. G. Black, 1990: The relationship of hurricane reconnaisance flight-level wind measurements to winds measured by NOAA's oceanic platforms. *J. Wind Eng. Ind. Aerodyn.,* **36,** 381–392.

Snyder, R., F. W. Dobson, J. A. Elliott, and R. B. Long, 1981: Array measurements of atmospheric pressure fluctuations above surface gravity waves. *J. Fluid Mech.,* **102,** 1–59.

Sterl, A., G. J. Komen, and P. D. Cotton, 1998: Fifteen years of global wave hindcasts using winds from the European Centre for Medium-Range Weather Forecasts reanalysis: Validating the reanalyzed winds and assessing the wave climate. *J. Geophys. Res.,* **103,** 5477–5492.

Swail, V. R., M. Parsons, B. T. Callahan, and V. J. Cardone, 1995: A revised extreme wave climatology for the east coast of Canada. *Proc. Fourth Int. Workshop on Wave Hindcasting and Forecasting,* Banff, AB, Canada, Atmospheric Environment Service, 81–91.

Thompson, E. F., and V. J. Cardone, 1996: Practical modeling of hurricane surface wind fields. *J. Waterway, Port, Coastal, Ocean Eng.,* **112** (4), 195–205.

WAMDI Group, 1988: The WAM model—A third generation ocean wave prediction model. *J. Phys. Oceanogr.,* **18,** 1775–1810.

Wu, J., 1982: Wind-stress coefficients over the sea surface from breeze to hurricane. *J. Geophys. Res.,* **87,** 9704–9706.